Fusion Engineering and Design 215 (2025) 114945

Contents lists available at ScienceDirect

Fusion Engineering and Design

journal homepage: www.elsevier.com/locate/fusengdes

Hydrogen explosion risk for EU-DEMO reactor considering tungsten dust reaction with steam

Tommaso Glingler [a,*], Danilo Nicola Dongiovanni [b], Gianfranco Caruso [a], Matteo D'Onorio [a]

[a] Sapienza University of Rome, Nuclear Engineering Research Group, Dipartimento di Ingegneria Aeronautica Elettrica ed Energetica (DIAEE), C.so Vittorio Emanuele II 244, 00186 Rome, Italy

[b] ENEA, Nuclear Fusion and Safety Technologies Department, via Enrico Fermi 45, Frascati 00040, Italy

ARTICLE INFO

Keywords:
EU-DEMO
WCLL
VVPSS
Hydrogen risk
MELCOR

ABSTRACT

Research activities in the Safety and Environment work package of EUROfusion, are carried out to evaluate structure system and components failure that could compromise the integrity of the confinement barrier and cause the release of contaminants for the European DEMOnstration (EU-DEMO) reactor. In this framework, deterministic safety analyses are performed to study the consequences of a postulated initiating event and determine whether such a failure event is bound within the safety objectives established for the plant. This paper studies the hydrogen explosion risk for the reference EU-DEMO reactor and evaluates the capability of new engineering safety system, such as passive auto-catalytic recombiner and exhaust detritiation system venting lines integrated with the vacuum vessel pressure suppression system, to minimize explosion risk by reducing hydrogen inventory in the atmosphere mixture.

The present study was carried out using the MELCOR 1.8.6 system code modified for fusion applications. The reference postulated initiating event selected for this study combines a small loss of vacuum accident and a small break loss of coolant accident. This scenario is characterized by two concurrent events with possibly explosive oxygen–hydrogen mixture formation. The ingress of air from the loss of vacuum breach provides a significant amount of oxygen, while the release of steam, because of the loss of coolant accident, results in an increase of hydrogen inventory by means of tungsten oxidation reactions. Such tungsten-steam reactions may occur either on plasma-facing hot surfaces or with tungsten dust, which recent studies highlighted as possibly playing a predominant role in hydrogen production. An external script has been developed to evaluate tungsten dust oxidation since a detailed model of such phenomenon is not currently present in MELCOR 1.8.6. First results highlighted that oxygen–hydrogen mixture reaches explosive limits inside the tanks of the vacuum vessel pressure suppression system. For this reason a new model of the vacuum vessel pressure suppression system with passive autocatalytic recombiners is studied to understand if the hydrogen explosion risk is mitigated.

1. Introduction

The pre-conceptual design phase of the EU-DEMO [1] reactor is actively supported by the Safety and Environment (SAE) work package of EUROfusion with safety analysis [2]. Elementary failures that have been indicated as safety relevant have been determined and grouped based on similarity of consequence and mitigating actions [3]. These failures are labeled as postulated initiating event (PIE) which should be investigated in terms of consequence by numerical analysis with system codes and Computational fluid-dynamics (CFD) simulations.

The system code currently adopted within EUROfusion to study consequences of failure event in terms of thermal-hydraulic and radionuclide transport is MELCOR version 1.8.6 for fusion applications [4]. The development of system codes for nuclear reactors has largely focused on light water reactor (LWR) technology, which means these codes are primarily equipped with fission-specific models. However, accident sequences in fusion reactors differ significantly from those in fission reactors, involving phenomena that is not present in fission-related accident scenarios. Therefore, Idaho National Laboratories (INL) has implemented a modified version of MELCOR 1.8.6 that incorporates physics relevant to a fusion power plant environment [5]. Modifications of the standard MELCOR code include steam oxidation models for PFC materials such as Berillium, and Tungsten. Other modifications include water freezing models representative of accident sequences involving cryogenic fluids. Most importantly radionuclide transport of tritiated water (HTO) is currently present in MELCOR 1.8.6 fusion version.

* Corresponding author.
E-mail address: tommaso.glingler@uniroma1.it (T. Glingler).

https://doi.org/10.1016/j.fusengdes.2025.114945
Received 29 November 2024; Received in revised form 28 February 2025; Accepted 5 March 2025
Available online 18 March 2025

Preliminary safety analysis of both Breeding Blanket (BB) concepts currently under investigation for the EU-DEMO reactor have been done with the MELCOR 1.8.6 fusion version. Concerning the Helium Cooled Pebble Bed (HCPB) BB, preliminary safety analysis have studied in-vessel LOCA and in-box LOCA [6]. For the in vessel LOCA, results have shown that the current sizing of the VVPSS is adequate to maintain the over-pressure below the safety limit [6].

Safety analysis of WCLL BB are also ongoing. In [7] an in-vessel LOCA of FW channels is studied. The simulation explores thermal-hydraulic behavior and radioactive release effects under two conditions: with and without isolation valve closures, located downstream of pump system. The VV pressure increases to about 0.15 MPa, but remains below the 0.2 MPa design pressure limit due to the VVPSS, minimizing off-site radioactive releases. Key findings indicate that dust, activated corrosion products (ACP), and HTO are entrained in steam and directed towards the VVPSS tanks. Closing isolation valves located downstream the primary pumps reduces ACP entry into the VV by 33%, though it also slows mobilization to suppression tank (ST)s due to reduced steam flow. Another sequence focus on the analysis of an ex-vessel LOCA from the first wall primary heat transfer system (FW-PHTS) hot ring in the upper pipe chase (UPC) [8]. Three nodalization models of the Tokamak building are compared in terms of pressure transients and unfiltered releases. Results indicate that the maximum Tokamak building pressure equal to 4.46 bar occurs in the UPC, with minor differences across models. A relief flow area of 16 m^2 connecting the UPC to primary heat transfer system (PHTS) room building is required to keep pressure below 2 bar, while a spray system (15 m^3/s at 20° C) effectively reduces peak pressures under 2 bar, significantly lowering unfiltered releases.

The current MELCOR 1.8.6 fusion version addresses several fusion safety issues to support the preliminary accident analysis of EU-DEMO. Nevertheless, modeling needs have been highlighted to cover phenomena more typical of fusion reactors, occurring during transient conditions [9]. A recent development of fusion-specific models for MELCOR has been done in [10]. This study addresses the mobilization of dust particles, which is particularly critical in fusion reactor environments where PFC erode over time. A resuspension model to accurately predict dust behavior and mitigate associated safety risks in accident scenarios within fusion reactors has been developed in MELCOR. Another significant advancement has been the integration of MELCOR with TMAP4, referred to as MELCOR-TMAP [11]. TMAP can model tritium diffusion, trapping, and permeation processes across reactor materials. This model is especially relevant for the safety management of the tritium fuel cycle in fusion reactors and for the BB, as it addresses permeation through materials and potential accumulation within the system's containment boundaries, helping to prevent tritium leakage and associated safety risks.

The effort of considering bounding case accident sequence for the EU-DEMO reactor and advancing the development of models for fusion system codes is the main topic of this paper. The PIE studied is a LOVA for the WCLL blanket concept. The breach is located at the interface between the VV lateral and the vertical shaft (VS). Air flows inside the VV, causing an unmitigated plasma disruption affecting the FW and thus causing the break of FW channels. The area of the breach and the number of FW channels involved are varied. Four different cases are analyzed and compared. This sensitivity study has been implemented to understand which combination of LOVA and LOCA area is worst in terms of hydrogen risk. As previously mentioned MELCOR evaluates the oxidation rate of the metallic heat structures, but a model which evaluates the oxidation of tungsten dust with steam is not available in MELCOR. For this reason, an external Python script has been developed and coupled with MELCOR to account for the hydrogen being produced from tungsten dust oxidation. The model contains two routines, the first one models the oxidation and the second one models an average specific surface area of the population of tungsten dust particles assumed. First results confirm that the principal mechanism of oxidation comes from tungsten dust.

The main result of the simulation is that explosive mixtures are reached inside the small leakage tank of the VVPSS. The BUR package of MELCOR models deflagration of gas mixture and in the accident investigated in this manuscript deflagration occurs inside the small leakage tank. The highest pressure is reached for Case 1 in the small leakage tank, equal to 2.1 bar. The deflagration could cause further damage to the E-DS lines connected to the small leakage tank and radiological contaminants could be released into the building room. For this reason in the final section of this paper another case study has been investigated to mitigate the risk of hydrogen explosion. The baseline model of the VVPSS is modified to include separate expansion tank (ET) with PARs. This suggested modification of the VVPSS reduces the amount of hydrogen that builds up in the atmosphere of the tanks. Results of this new model of the VVPSS with PARs demonstrate that hydrogen explosion is avoided.

2. Materials and methods

2.1. Overview of the EU-DEMO water cooled lead lithium breeding blanket

The design of EU-DEMO reactor taken as a reference for the safety analysis of this paper is the WCLL BB concept based on DEMO2017 baseline [12], with a fusion power of about 2 GW. A detailed description of the WCLL design and the integration with systems interfaced is presented in [13].

The BB is a critical component for the successful operation of a commercial fusion power plant. Tritium breeding and heat extraction from the plasma are both functions of a BB system. For the WCLL concept heat extraction is accomplished by a pressurized water loop at PWR thermal-hydraulic conditions equal to 15.5 MPa. The breeding of tritium instead is done though neutron capture of Li6, present as an Lead Lithium eutectic alloy.

Directly interfaced with the plasma, the WCLL BB is an in-vessel component divided into 16 sectors positioned along the toroidal direction. Each sector is separated in 3 OB and 2 InBoard (IB) segments (Fig. 1).

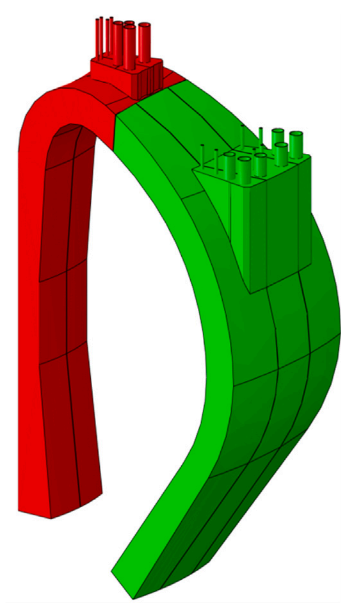

Fig. 1. EU-DEMO sector of the water-cooled lead-lithium breeding blanket with two inboard and three outboard segments.

Around 100 breeding cells distributed along the poloidal direction made up a single segment [13]. The water cooling circuit and the Lead Lithium loop are interfaced inside the breeding cell. The section of the cell that faces the plasma chamber, called FW is made up of a 2 mm thickness layer of Tungsten and 7 × 7 mm water cooled squared channels. The inside of the cell, called the breeding zone (BZ) is a squared box containing Lead Lithium which is crossed radially by water double wall tubes (DWTs), (Fig. 2).

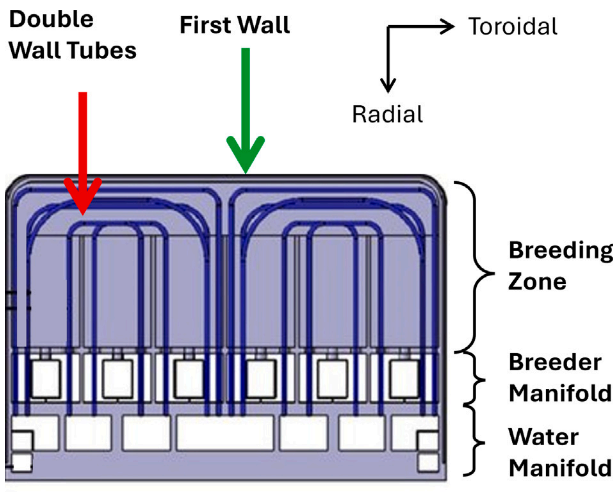

Fig. 2. WCLL2018.v0.6 OB equatorial cell: poloidal-toroidal view.

Manifolds are present in each sector to collect and distribute water of squared channels and DWTs. The design of the PHTS adopted for this analysis is made up of two water coolant loops, the FW-PHTS which is connected to manifolds of the squared channels of the breeding cell and the breeding zone primary heat transfer system (BZ-PHTS) which instead is connected to the DWTs subsystem. Both PHTS distribution and collector rings of the water cooling loop run outside of the VV along toroidal direction. FW-PHTS and BZ-PHTS are independent having each a pressurizer, pump system and once through steam generator (OTSG). Main parameters of the WCLL BB system are reported in Table 1.

Table 1
VVPSS system parameters.

Parameter	Units	Value
Pressure	MPa	15.5
Temperature range	°C	295–328
Av. Coolant density	kg/m^3	701.3
FW-PHTS flow rate	kg/s	2273.6
BZ-PHTS flow rate	kg/s	7662.4
FW water inventory	m^3	179.2
BZ water inventory	m^3	501.5

Regarding the radiological contaminants of the WCLL the main contents are tritiated water, in the form of HTO and ACP. Tritium permeates through the structures of the BZ from the lead lithium loop to the water cooling loop. Several studies are ongoing in EUROfusion to estimate the tritium concentration inside the water cooling loops of the FW and BZ. A preliminary value considered in the pre-conceptual design phase of DEMO is equal to 0.015 g/m^3 [2] taken from past experience of CANDU reactors [14] and adopted to specific thermal-hydraulic conditions of the PHTS. Conversion factor between tritium and HTO is 6.63 and considering a total water inventory of the whole WCLL equal to 680.7 m^3 gives a total amount of 67.8 g – HTO. Analysis are ongoing to evaluate the correct amount and the value presented in this paper is not definitive.

Just as in water cooled reactors, the corrosion of activated piping and components of the cooling system releases ACP in the cooling circuit. The estimated ACP deposit mass is approximately 10 kg, while the ACP mass present in the coolant, including ions and cruds, is around 20 g [15].

2.2. Overview of the EU-DEMO building model

The building room containing the primary heat transfer system distributor and collector ring is called the upper pipe chase, and is connected to the vertical shaft and the lower pipe chase. The three environments are grouped together in the so called tokamak containment room. Main components like PHTS pump, pressurizer and once through steam generator are instead in a separate compartment called the PHTS vault [16]. The top maintenance hall is used for maintenance activities such as removing in vessel components and it is positioned on top of the tokamak containment rooms. The EU-DEMO building and rooms are shown in Fig. 3.

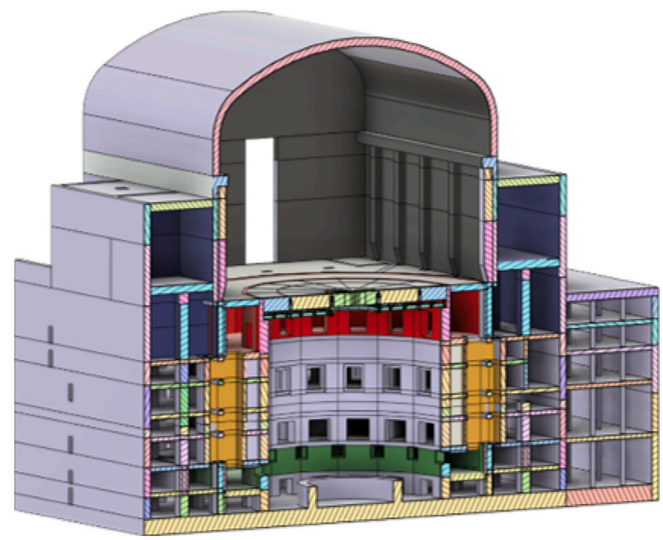

Fig. 3. EU-DEMO building and rooms.

2.3. Vacuum vessel pressure suppression system

The primary confinement barrier against the release of radiological contaminants is the VV. The current pressure design limit of the VV has been set at 0.2 MPa. In case of an in-vessel LOCA the integrity of the first safety barrier could be compromised. Due to the enthalpy content of the BB, without the intervention of a mitigation system or venting the pressure design limit could be overcome. Therefore, the system designed to adequately mitigate over-pressure transient inside the VV is the VVPSS. The concept behind the VVPSS is to convey external energy sources to dedicated water suppression tanks, thus suppressing the energetic content being release from in-vessel LOCA.

A preliminary sizing of the VVPSS has been done in [17], the first step consisted on the definition of the water content of the suppression tanks. Tank inventory is designed to satisfy the first safety objective of the system which is to obtain a equilibrium pressure of the VV equal to 0.1 MPa in case of ingress of LOCA event. The second safety objective is to limit the pressure peak under the design limit, which drove the sizing of a relief area and opening set point. The result of the preliminary design of the VVPSS, as shown in Fig. 4, consists on one tank dedicated to leakages called small leakage tank (SLT) actuated by a BL valve, four tanks which suppress steam in case of in-vessel LOCA called ST actuated by RD. Main parameters of tank inventory, opening relief area and set point are summarized in Table 1 and Table 2.

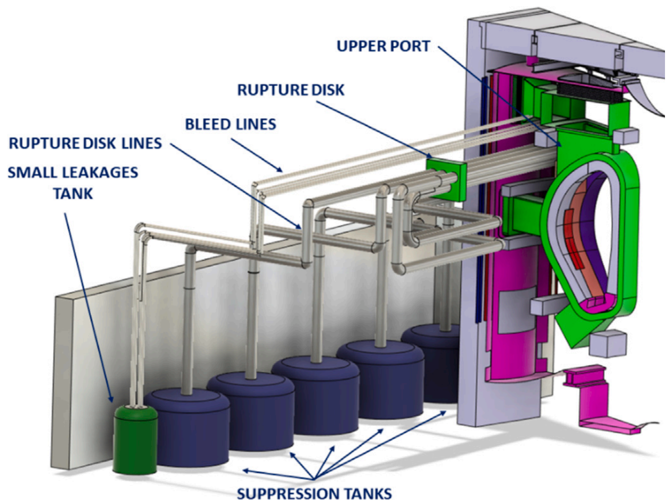

Fig. 4. Vacuum Vessel Pressure Suppression System layout [18].

Table 2
VVPSS system parameters.

Parameter	Units	Value
RD relief area	m^2	1.6
RD set point	kPa	150.0
BL relief area	m^2	0.6
BL set point	kPa	90.0
ST volume	m^3	500.0
ST pool fraction	–	0.6
ST initial pressure	Pa	9600.
ST initial temperature	K	303.0
SLT volume	m^3	300.0
SLT pool fraction	–	0.6
SLT initial pressure	Pa	9600.0
SLT initial temperature	K	303.0

3. Modeling

3.1. MELCOR model

The MELCOR input deck adopted for this analysis has been described in previously published research papers [7,8,18,19]. Main assumptions and details of the WCLL BB, the EU-DEMO environments and the VV models developed in MELCOR are presented in [8]. Nevertheless, the MELCOR model of this paper has some improvements to account for the specific phenomena occurring in the accident studied. Next sections provide a description of the motivations and changes done to the model described in [8].

3.1.1. PFC heat structure modeling for hotspots

A modification to the heat structure model of the in-vessel components has been done to evaluate potential issues related to hotspots. Hydrogen generation resulting from the oxidation of tungsten has been studied in [20]. Results are presented also in terms of tungsten temperature influence on hydrogen generation rate, becoming significant at temperatures exceeding 1060.0 K. Therefore, high-temperature hotspots are the primary contributors to hydrogen generation. Following this consideration, the VV surfaces were divided into sections (a_i) to account for hotspot regions. Table 3 shows the area division of the FW and Divertor heat structure to model hotspots.

The heat structures of hotspots surfaces have been modeled with a convective boundary condition on the side facing the VV control volume; while the other side of the heat structures have a convective boundary condition with a cooling channel of the FW or Divertor.

Table 3
Area division of FW and Divertor, hotspots and relative initial temperature.

Heat structure of:	a_i (%)	Area (m^2)	Initial Temp. (K)
	a_1 = 50	734.9	673.15
	a_2 = 35	514.43	823.15
	a_3 = 10	146.98	973.15
FW Area = 1469.8 m^2	a_4 = 4	58.79	1223.15
	a_5 = 0.99	14.55	1473.15
	a_6 = 0.009	0.13	1723.15
	a_7 = 0.001	0.015	1973.15
	a_1 = 50	65.1	673.15
	a_2 = 35	45.57	823.15
	a_3 = 10	13.02	973.15
Divertor Area = 130.2 m^2	a_4 = 4	5.208	1223.15
	a_5 = 0.99	1.29	1473.15
	a_6 = 0.009	0.011	1723.15
	a_7 = 0.001	0.0013	1973.15

3.1.2. Vacuum vessel pressure suppression system MELCOR model

The main difference between the baseline line MELCOR model and the input deck used for the analysis of this paper is associated with the implementation of the E-DS connected to the tanks of the VVPSS. The tanks have a connection towards the E-DS for venting, to collect radiological contaminants and remove H_2 in the atmosphere, reducing the risk of detonation in the tanks. Preliminary data assumed for the E-DS flow rate is equal to 1400.0 m^3/h per line, while the pipe diameter are assumed equal to 10 cm. The preliminary data used to model the E-DS are assumed from EU-DEMO Safety Data List and are still in development. Detritiation values are associated to the amount of tritium which can be recovered from streams by the E-DS. Main values of the E-DS are:

- Filter effectiveness η:
  - η > 99% detritiation (due to initial condensation in condenser with minimum reduction of the exhaust humidity by factor of 10)
  - η > 99.9% ACP/dust filter
- Triggered at reaching:
  - ST pressure of 90 kPa with 3 min delay (to open valve), or
  - VV pressure of 95 kPa
- Closed at reaching:
  - VV pressure under 90 kPa
  - ST pressure under 50 kPa

The MELCOR model includes the E-DS lines connected to the STs and small leakage tank. Since the analysis focuses on the risk of H_2 detonation and deflagration the lines are also included in the modeling. The model consists on two collectors for the piping of the E-DS, one for the small leakage tank and one for the STs. Each tank is connected to the collector with a vertical pipe. Fig. 5 shows the MELCOR model of the VVPSS which considers, tanks and the E-DS piping, with corresponding valves.

The E-DS capacity of 1400 m^3/h, is modeled in MELCOR using a fixed velocity assigned to the flow path (FL) for the inlet and outlet of the main E-DS line shown in Fig. 5. Venting through the E-DS occurs when tank pressure exceeds the system's operating pressure.

The VVPSS model shown in Fig. 5 is used for a first analysis of hydrogen explosion risk. To further reduce the risk of hydrogen detonation, a suggested improvement to the VVPSS design involves incorporating PAR in dedicated ETs. Specifically, the small leakage tank connects to ET-A through a non-return valve, while the remaining ST connect to ET-B (Fig. 6).

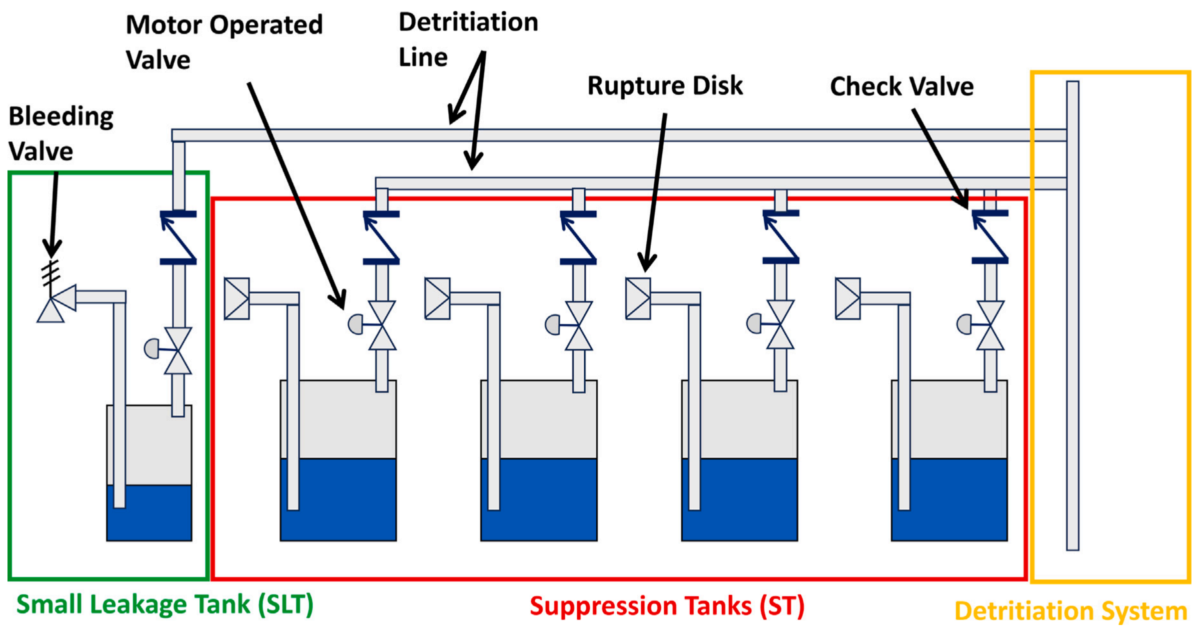

Fig. 5. Baseline VVPSS MELCOR model with E-DS.

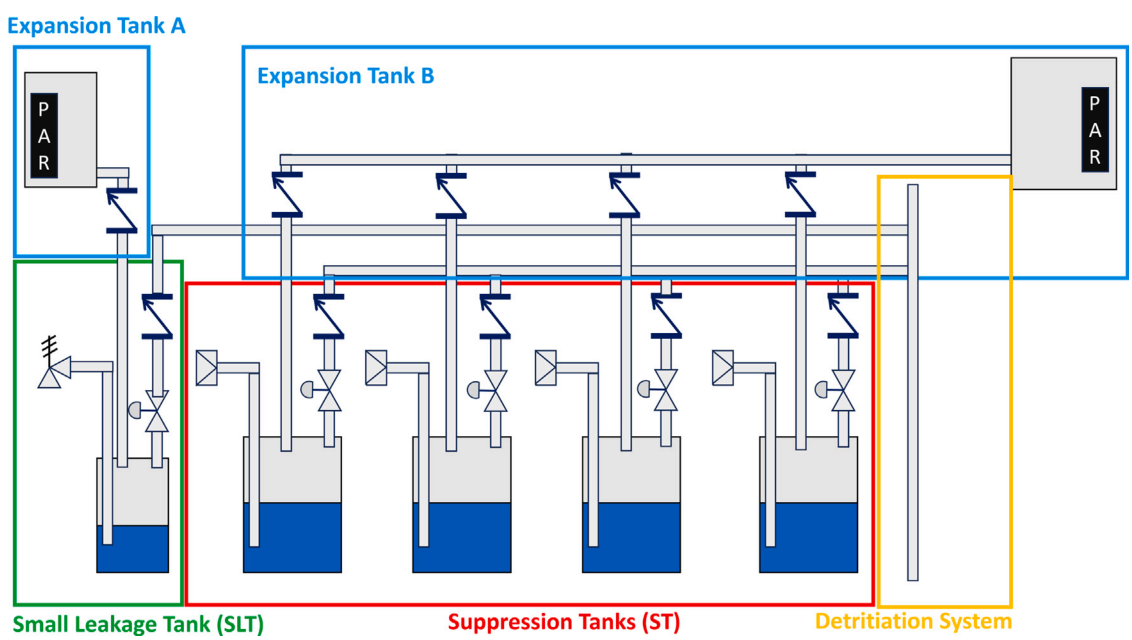

Fig. 6. Modified VVPSS MELCOR model with E-DS and PAR.

Table 4
BL and RDs set point for the baseline and optimize model.

MELCOR model	BL valve set point (kPa)	RD opening set point (kPa)	ET volume (m^3)
Baseline	90.0	150.0	–
Optimize	35.0	65.0	450.0

Following the results presented in [19], the VVPSS geometric and initial boundary conditions are adjusted to optimize hydrogen recombination. BL and RD set-points are modified compared to the baseline configuration. Table 4 outlines the key differences between the baseline model and the optimized VVPSS model featuring PARs in the ETs.

3.1.3. BUR MELCOR package

The main scope of the analysis is to quantify the risk of hydrogen explosion. Using Shapiro diagram a first graphical overview determines if the mixture composition reaches flammable conditions [21]. This graphical approach can be used to track the gaseous mixture inside the control volumes during the transient. Each point in the Shapiro diagram represents the mixture composition based on the volume concentration of H_2, air and inert gases. The combustion of gases instead is modeled in MELCOR by activating the BUR package.

The BUR package simulates gas combustion within control volumes [22], focusing on global effects rather than detailed reaction kinetics. Gases in the BUR model are considered premixed and tracking the actual flame front propagation is not considered. Deflagration are modeled while detonations are identified and flagged but are not actively simulated. Deflagration is initiated when the mole fraction composition in a control volume meet LeChatelier's formula. The following equations Eqs. (1), (2), (3), determine the threshold for ignition.

$$X_{H_2} + X_{CO}\left(\frac{X_{H_2,ign}}{X_{CO,ign}}\right) \geq X_{H_2,ign} \tag{1}$$

$$X_{O_2} \geq X_{O_2,ign} \tag{2}$$

$$X_{H_2O} + X_{CO_2} \leq XMSC_{ign} \tag{3}$$

X_{H_2}, X_{O_2}, X_{CO}, X_{H_2O}, and X_{CO_2} are hydrogen, oxygen, carbon monoxide, steam and carbon dioxide mole fraction in a control volume respectively. While the variables with subscript *ign* indicate the corresponding compound mole fraction limit for ignition. $XMSC_{ign}$ is the maximum diluent mole fraction for ignition. Therefore, burn in a control volume of MELCOR is initiated when all three equations Eqs. (1), (2), (3) are satisfied. The user can modify the ignition limit default values (set at $X_{H_2,ign} = 0.10$, $X_{O_2,ign} = 0.05$ and $XMSC_{ign} = 0.55$).

When ignition occurs, the model takes into account combustion completeness, burn duration, combustion rate with correlations derived experimentally. Flame propagation to connected volumes is evaluated considering a propagation delay time. This delay takes into account the time needed for a flame to reach the edge of a control volume.

With the current assumptions described above accumulation of hydrogen is not possible since as soon as the three criteria are met ignition occurs. This approach is not conservative because ignition of a higher volume concentration of hydrogen would provoke a higher amount of energy. Furthermore, unrealistic burning of gases would occur with consecutive ignition and flame extinction. Due to the different rate of hydrogen generation and burn, ignition would be triggered several times in the same control volume.

To overcome these drawbacks, the $X_{H_2,ign}$ limit has been increased and set at 0.18% to model accumulation of hydrogen and avoid multiple deflagration inside the same volume. The high ignition limit of H_2 considered can have as a consequence a deflagration to detonation transition in small volumes. The volumes considered in the analysis, such as the VV and the VVPSS tanks, are characterized by a high volume and this risk is avoided. Future studies should consider a parametric analysis on the value associated to the ignition limit. Nevertheless, main scope of the BUR package is not to evaluate if ignition occurs inside a control volume, rather it focuses on the consequences of igniting a mixture of gases which reaches deflagration conditions.

3.2. Python external model for tungsten dust oxidation

MELCOR has been modified by INL [23] for safety analysis of the International Thermonuclear Experimental Reactor (ITER). One of the updates is the oxidation model of fusion specific materials which evaluates oxidation of Beryllium, Carbon and Tungsten, described in detail [23]. The modifications of MELCOR allow to simulate oxidation phenomena of PFC when they are modeled as a heat structure using reaction rates obtained experimentally, but oxidation of metallic dust cannot be evaluated. To address this limitation, an external Python script has been developed and integrated with MELCOR to assess tungsten dust oxidation. The script accounts for variables such as particle size, partial pressure of steam and dust temperature to estimate hydrogen production and the heat generated by the chemical reaction.

The calculation procedure is structured as a two-step iterative process involving MELCOR and Python script exchanging feedback. To account for oxidation of tungsten dust, partial pressure of steam and temperature of tungsten dust has to be taken into account. These values are evaluated in the first step by MELCOR, and using external data file (EDF) output, partial pressure of steam and tungsten temperature can be read in the Python script. The output of the Python script is the hydrogen produced and the heat generated, and the results of Python are read by MELCOR in the next step of calculation through EDF.

The internal workflow of the Python script is divided in two routines. The first one is described in Section 3.2.1 which estimates the specific surface area. The second one is the chemical routine (Section 3.2.2).

3.2.1. Specific surface area routine

The specific surface area is an average value that characterizes the properties of an aerosol particle population. Based on [24], the lognormal distribution is considered the most appropriate for describing single-source aerosols. This distribution is defined by geometric standard deviation (GSD) and count mean diameter (CMD), assuming that particles are spherical, see Eq. (4). For this analysis tungsten dust is considered with a GSD of 2.0 and a CMD of 0.5 μm. Values are referenced from estimates of ITER dust, which predominantly consists of beryllium.

$$f(d_p) = \frac{1}{d_p\sqrt{2\pi}\ln(\sigma_g)}\exp\left\{-\frac{\left[\ln(d_p)-\ln(\text{CMD})\right]^2}{2\cdot\ln(\sigma_g)^2}\right\} \tag{4}$$

According to [25] the specific surface area can be derived from the diameter of particle with average mass (d_m) and the diameter of particle with average surface area (d_s):

$$d_m = \left(\frac{6m}{N\rho\pi}\right)^{\frac{1}{3}} \tag{5}$$

$$d_s = \sqrt{\frac{A_{tot}}{N\pi}} \tag{6}$$

where A_{tot} is the total surface area assuming that the inside surface area of the particles gives no contribution. N is the number of particles of the distribution derived as a function of the total inventory of the dust which is one of the boundary conditions of the problem.

$$N = \frac{6m}{\pi\rho\int f(x_p)x_p^3\,dx_p} \tag{7}$$

For EU-DEMO tungsten dust inventory is estimated between 690 kg and 1379 kg, depending on the frequency of the disruption occurrences. An average value of 1034 kg is assumed to be deposited on VV surfaces [15] for this analysis. The specific surface, A_s in m^2/g can therefore be derived from:

$$A_s = \frac{d_m^3}{\rho d_s^2} \tag{8}$$

3.2.2. Oxidation routine

The Tungsten dust reaction with steam is evaluated with the following reaction rate presented in [23] which took as reference the correlation derived experimentally from [20] and converted from liter/g to kg-W/m^2 s:

$$RR_w = \left(\frac{P_{H_2O}}{P_0}\right)^{0.78}\cdot 41.238\cdot\exp\left(-\frac{33106.0}{R\cdot T_W}\right) \tag{9}$$

where $P_0 = 0.84$ bar and R = 1.98 kJ/kg K; RRw is expressed kg_W/m^2 s, for a given temperature T_W and P_{H_2O}.

To estimate the mass of hydrogen produced during the reaction between tungsten and steam, the RR_W is multiplied by the specific surface area A_s of tungsten involved in the reaction and the time step of calculation. This calculation yields the reacted mass of tungsten, which can then be used to determine the mass of hydrogen produced using the chemical balance:

$$W + 3H_2O \rightarrow WO_3 + 3H_2 \tag{10}$$

4. Accident description and main results

The selected PIE for this study involves a combination of a small LOVA and a small LOCA. This dual scenario poses a risk of forming a potentially explosive oxygen-hydrogen mixture. From the tokamak containment rooms air enters through the LOVA breach, while the LOCA leads to steam release within the VV, inducing hydrogen production through tungsten steam oxidation reactions. MELCOR evaluates oxidation reactions which occur on PFC hot surfaces, while the external Python script estimates tungsten dust oxidation.

The VV inventory includes 2.6 kg of Tritium and 1.75 kg of Deuterium, with the latter amount calculated based on an equivalent molar quantity to Tritium. This inventory represents the total quantity of Tritium and Deuterium across all components, including PFCs, dust, pumps, and atmosphere. These values are evaluated under the conservative assumption that the all mass is located in the VV environment. Instead, tritium in the VV is divided between:

- immobilized in PFC which becomes mobilizable if desorbed by baking
- mobilized in dust

Previous ITER analysis have adopted a conservative assumption regarding tritium, stating that any mobilized tritium gas will be immediately oxidized and released in the form of HTO [23]. This assumption is based on the fact that HTO is significantly more radiotoxic compared to elemental tritium gas. However, for this analysis the scope is to quantify the risk of hydrogen explosion and in-vessel tritium is not considered as HTO. For assessing the risk of a hydrogen explosion, Tritium and Deuterium present in the VV are treated as equivalent to hydrogen in their contribution to potential explosive mixtures.

To increase the insights of the accident, a sensitivity analysis was conducted on the areas affected of the LOVA and LOCA. The aim is to identify the combination of LOVA and LOCA area that would increase the risk of a hydrogen explosion. Four distinct cases were selected for this purpose, with Table 5 providing data of each case and the corresponding LOVA and LOCA areas.

Table 5
Cases studied for the parametric analysis and corresponding values of LOVA and LOCA area.

Scenario ID	LOVA area m^2	LOCA area m^2
Case 1	2.0×10^{-3}	9.8×10^{-4} (10 FW channels)
Case 2	2.0×10^{-3}	9.8×10^{-3} (100 FW channels)
Case 3	2.0×10^{-2}	9.8×10^{-4} (10 FW channels)
Case 4	2.0×10^{-2}	9.8×10^{-3} (100 FW channels)

Results of the baseline model of the VVPSS are discussed in Section 4.1 and compared with an alternative design incorporating PARs connected to the VVPSS tanks which results are discussed in Section 4.2. This design aims to recombine hydrogen, reducing its accumulation in the tank atmospheres and mitigating the risks of hydrogen ignition.

4.1. Baseline case

The PIE occurs at 0.0 s involving a small breach that connects the VV to the Tokamak containment rooms, consisting in the upper pipe chase, the vertical shaft and the lower pipe chase. Air flows from the vertical shaft into the VV, resulting in a loss of vacuum. Ingress of air and impurities causes an unmitigated plasma disruption at 0.1 s, which leads to the rupture of FW channels. Coolant with a high enthalpy content is discharged into the VV and induces a pressurization transient (Fig. 7).

The VVPSS intervenes to mitigate the pressurization trend. Set point of the bleeding valve is at 90.0 kPa while the rupture disks set point is at 150.0 kPa. The pressure transient behavior differs across the four cases studied. Since cases 1 and 3 feature smaller rupture areas, the pressure increases slower compared to Cases 2 and 4, which instead involve larger LOCA areas. Nevertheless, the pressure transient of the VV volume reaches the opening set point of the rupture disks for all cases, and in the long term the LOCA is safely mitigated by the intervention of the VVPSS.

Figs. 8 and 9 show the pressure transient behavior of the small leakage tank, and of the suppression tank, where steam is suppressed.

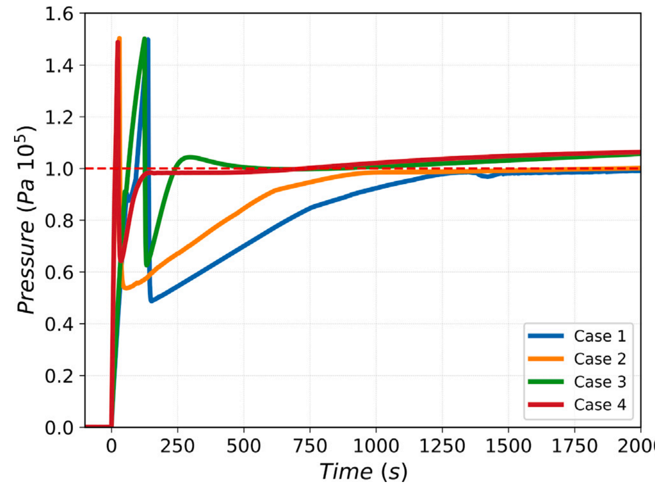

Fig. 7. Pressure transient of VV volume.

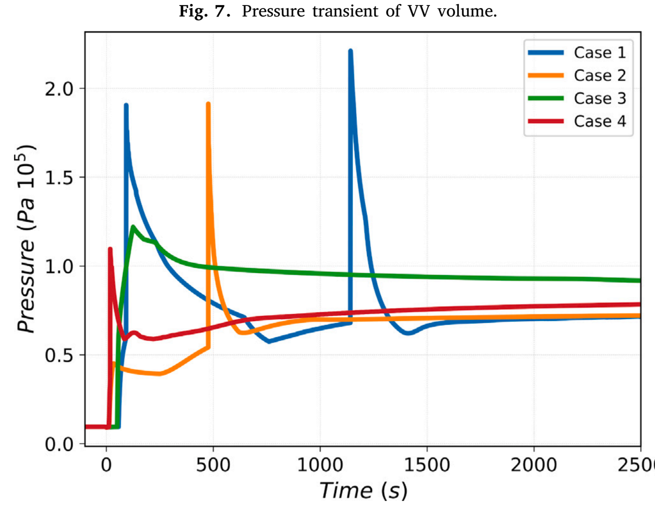

Fig. 8. Small leakage tank pressure transient.

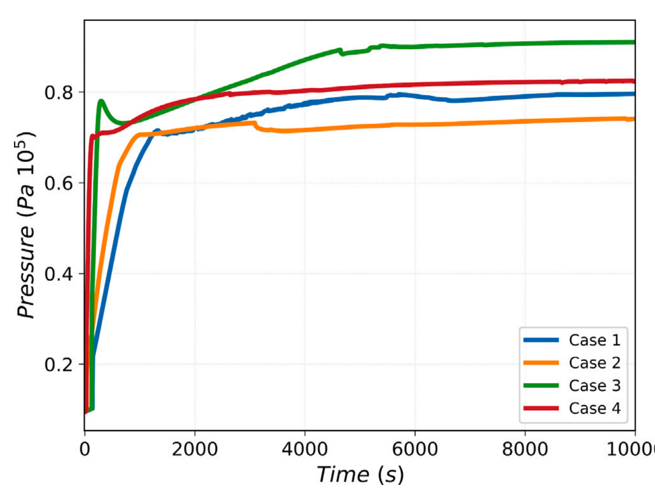

Fig. 9. Suppression tank B pressure transient.

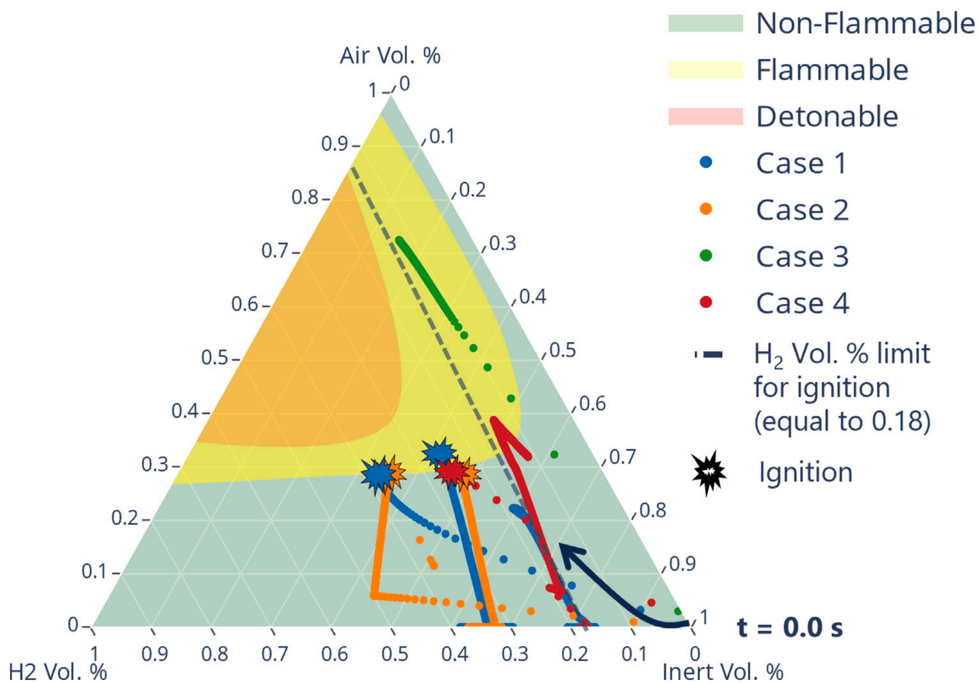

Fig. 10. Shapiro diagram representing for the small leakage tank.

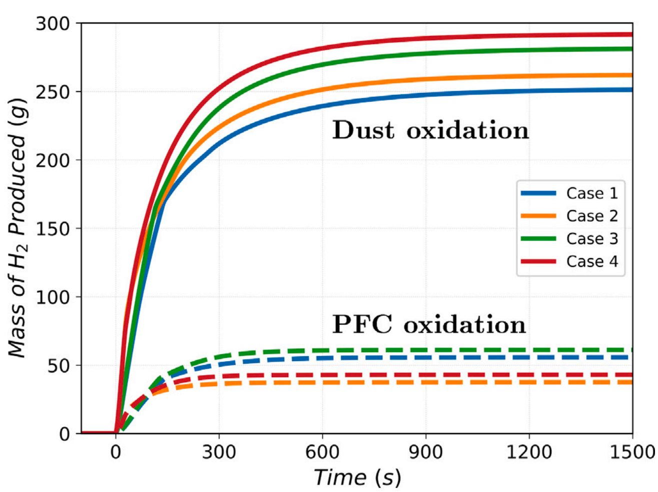

Fig. 11. Comparison between amount of H_2 produced by tungsten dust and PFC oxidation.

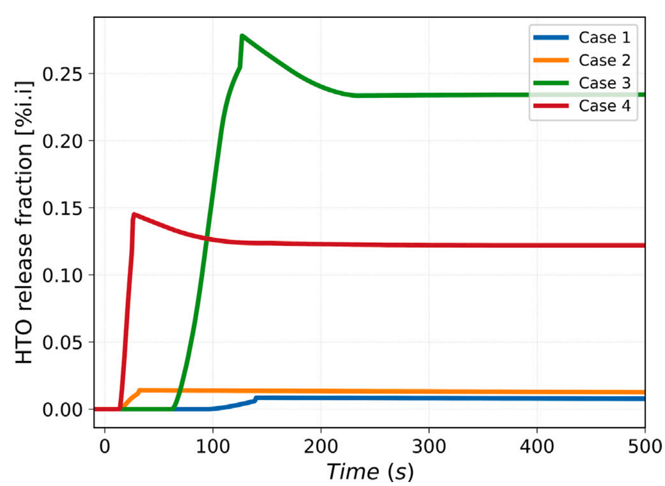

Fig. 12. HTO release fraction in % of initial inventory to the TCR.

The suppression of steam in the small leakage tank does not effectively slow the pressurization of the VV, until the rupture disk set point of 150.0 kPa is reached. Once the rupture disks open, significant amounts of steam are discharged from the VV to the suppression tanks (ST-B to ST-E). This process results in a rapid pressure drop within the VV, followed by a gradual increase as equilibrium is established with the connected tokamak containment rooms.

The pressure transient in the small leakage tank is influenced by the combustion of premixed gases. The pressure peaks represented in Fig. 8 are associated to deflagration of H–O mixture. The Shapiro diagram for the small leakage tank is shown in Fig. 10, and shows ignition of flammable mixtures in Case 1, Case 2 and Case 4. Case 3 reaches flammable conditions, yet it does not satisfy the ignition requirement of H_2 vol. % higher 0.18%. Instead, ignition occurs twice in Case 1, producing the highest peak pressure compared to the other cases. Combustion of premixed gases in the small leakage tank poses a risk of potentially compromising the safety function of radiological containment since most of the HTO is discharged towards the VVPSS.

Venting of small leakage tank is open during the deflagration allowing flame propagation towards the E-DS lines. For Case 1 and Case 2 flame propagation is simulated while instead is absent for Case 4. Table 6 outlines peak pressures in the small leakage tank and in the E-DS line.

As a preliminary result of the hydrogen explosion risk assessment, Case 1 which is characterized by the smallest LOVA and LOCA area, has the highest consequence in terms of pressure peak due to hydrogen explosion. Instead, Case 4 which is characterized by the higher LOVA and LOCA area, has the lower risk in term of hydrogen explosion.

The total H_2 produced from oxidation of tungsten PFC and dust is shown in Fig. 11 estimated by MELCOR and Python script. Preliminary results indicate that the primary source of H_2 is the reaction of tungsten dust with steam. This is attributed to an average high specific surface area of dust equal to 189.3 m^2/kg.

Due to the in-vessel LOCA, releases of HTO from the primary confinement towards the tokamak containment rooms are shown in Fig. 12 in terms percentage of initial inventory.

In the early phase of the accident, air flows into the VV from the LOVA breach due to the lower VV pressure relative to the tokamak containment rooms. When the pressure of the VV overcomes the tokamak containment rooms pressure, air flow through the LOVA breach is reversed and HTO is released from the primary confinement barrier. Results show that most of the radiological contaminant is instead discharged towards the VVPSS tanks reaching around 40% of i.i. and the remaining is contained in the VV.

Table 6
Pressure peak values for different cases.

Scenario ID	Pressure peak in (bar) of	
	SLT	E-DS
Case 1	2.21	1.92
Case 2	1.91	2.62
Case 3	1.22	1.12
Case 4	1.09	0.99

4.2. Vacuum vessel pressure suppression system with passive autocatalytic recombiners case

In this section the accident sequence studied has a different design of the VVPSS. PARs are installed in dedicated expansion tanks to mitigate the hydrogen explosion risk. The model has also different opening set point of the bleeding line, equal to 30.0 kPa, and the rupture disks, equal to 65.0 kPa. The set point values have been retrieved from an optimization study presented in [19].

Fig. 13 shows the short-term pressure behavior of the plasma chamber for the different cases. Case 1 and Case 3 have a similar transient due to the equal LOCA area assumed, and differ from Case 2 and Case 4 affected by the rupture of 100 FW channels. For all cases the discharge of steam towards the VVPSS tanks safely mitigates the LOCA. Case 1 and Case 2 are

Fig. 14 shows the pressure transient for the small leakage tank. The different set-point of the BL and RDs lead to a reduction of the pressure transient within the small leakage tank, maintaining it below the operating pressure of the E-DS and venting is no longer triggered. This consequence is associated also to the opening of connections towards the expansion tanks. Compared to the analysis presented in Section 4.1, pressure peaks associated to deflagration are no longer present for the exception of Case 1.

Ignition of the H-O mixture can also be seen in the Shapiro diagram, Fig. 15 relevant for the small leakage tank. The resulting pressure peak from the deflagration in Case 1, does not pose a significant safety risk as shown in Fig. 14. In the other cases, while the gaseous mixture reaches flammable conditions (Fig. 15), the hydrogen volume concentration remains below the ignition threshold.

Hydrogen recombination inside the ET due to PAR operation decreases the amount of hydrogen accumulated in the atmosphere of the VVPSS tanks, reducing therefore the risk of deflagration of H-O mixtures. As soon as steam is discharged towards the VVPSS, the lines

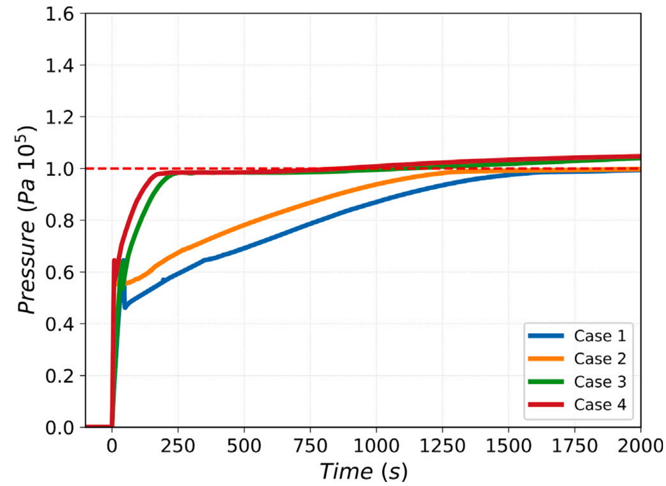

Fig. 13. Pressure Transient of VV volume.

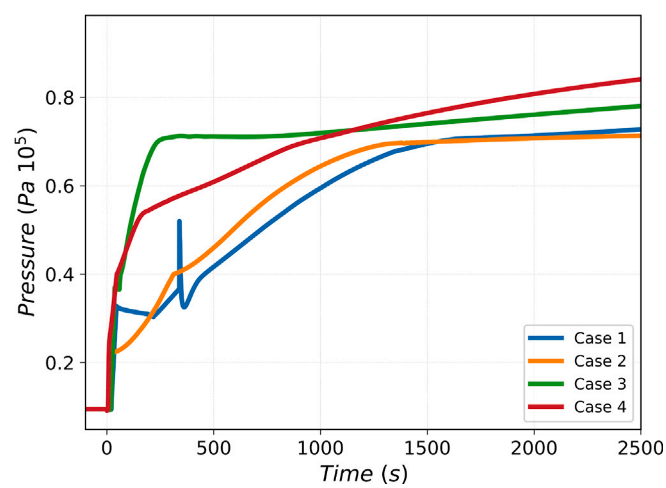

Fig. 14. Small leakage tank pressure transient.

connecting the small leakage tank and the suppression tanks to the ET open. In Fig. 16 the total mass of H_2 recombined by both the PAR units installed in the two dedicated ET tanks is shown. The highest value of H_2 recombined are associated with Cases 2 and Cases 4. This result is caused by a higher amount of hydrogen discharged towards the ET for Case 2 and Case 4 compared to the remaining cases. Inside the ET, the PAR unit recombines hydrogen following the equation described in [19]. Operation of the PAR unit is started when the vol. concentration of H_2 is higher than 2% and the temperature is above 50 °C.

As a conclusion of the case studied in Section 4.2, the hydrogen explosion risk is greatly reduced, only for Case 1 deflagration occurs. The main event which leads to a decrease of hydrogen accumulation in the VVPSS tanks is associated to the hydrogen recombination, as shown in Fig. 16. This brings a benefit in the first part of the transient avoiding deflagration compared to the baseline case presented in Section 4.1.

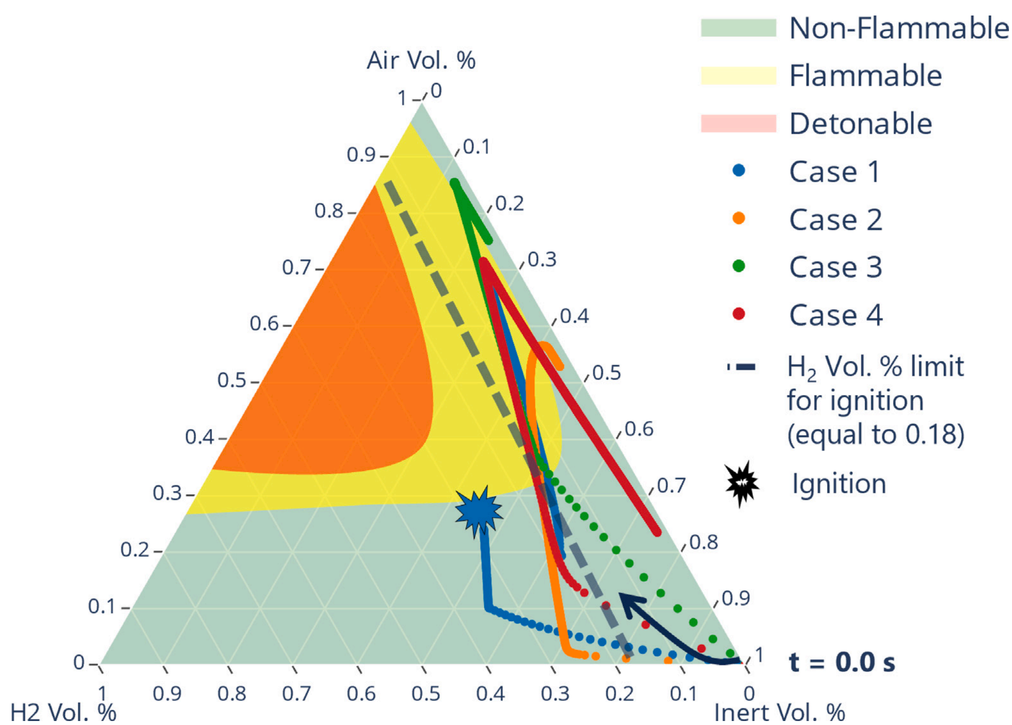

Fig. 15. Shapiro diagram representing the mixture of gases present in the small leakage tank.

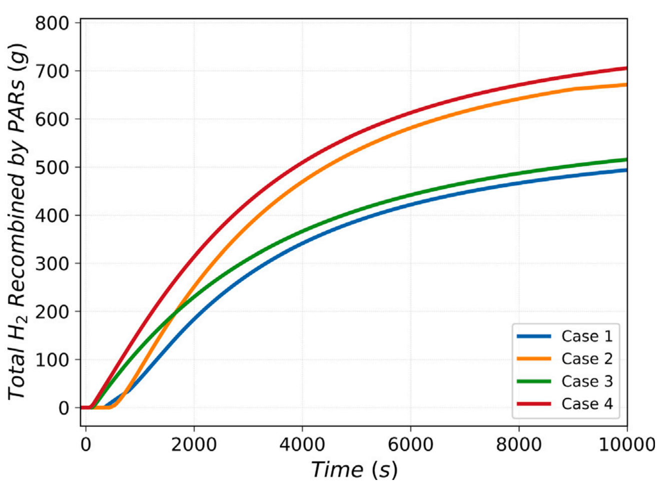

Fig. 16. Integral mass of H_2 recombined in the PARs.

5. Conclusions

The design of EU-DEMO reactor is advancing from the conceptual phase to a more detailed stage, with systems being developed in alignment with their assigned functional criteria. Safety analysis plays a key role in supporting and evaluating the ongoing design while identifying potential criticality that could lead to adverse consequences during accident scenarios.

Within this context, a hydrogen explosion risk assessment has been conducted for a scenario involving a LOVA followed by the rupture of a FW channel, leading to an in-vessel LOCA. The results indicate that the VVPSS effectively mitigates the pressure rise associated with this accidental sequence. However, the simultaneous ingress of air and generation of hydrogen introduces a significant risk of forming flammable mixtures. An external Python script has been coupled with MELCOR to evaluate also the contribution of tungsten dust oxidation in the hydrogen production. First results show that the main source of hydrogen production might come from tungsten dust oxidation rather than PFC oxidation.

Simulations based on the current VVPSS design predict the formation of a flammable mixture within one of the VVPSS tanks and if ignited, flame propagation reaches also the E-DS lines connected to it. This deflagration could cause an overpressure capable of further damaging the containment and potentially leading to the release of water containing HTO.

To address this risk, a modified VVPSS design incorporating separate ET equipped with PARs has been evaluated. This solution has been demonstrated to effectively prevent hydrogen deflagration, thereby enhancing safety and mitigating the associated risks.

CRediT authorship contribution statement

Tommaso Glingler: Writing – review & editing, Writing – original draft, Visualization, Software, Methodology, Investigation, Formal analysis, Data curation, Conceptualization. **Danilo Nicola Dongiovanni:** Writing – review & editing, Supervision, Formal analysis, Conceptualization. **Gianfranco Caruso:** Writing – review & editing, Supervision, Formal analysis, Conceptualization. **Matteo D'Onorio:** Writing – review & editing, Writing – original draft, Methodology, Formal analysis, Conceptualization.

Declaration of Generative AI and AI-assisted technologies in the writing process

During the preparation of this work, the author(s) used the OpenAI GPT-4 language model, commonly known as ChatGPT, in order to improve the clarity and structure of English writing, as well as to assist with formatting tasks. After using this tool/service, the author(s) reviewed and edited the content as needed and take(s) full responsibility for the content of the publication.

Declaration of competing interest

The authors declare that they have no known competing financial interests or personal relationships that could have appeared to influence the work reported in this paper.

Acknowledgments

This work has been carried out within the framework of the EUROfusion Consortium, funded by the European Union via the Euratom Research and Training Programme (Grant Agreement No 101052200 EUROfusion). Views and opinions expressed are however those of the authors only and do not necessarily reflect those of the European Union or the European Commission. Neither the European Union nor the European Commission can be held responsible for them.

Data availability

Data will be made available on request.

References

[1] G. Federici, J. Holden, C. Baylard, A. Beaumont, The EU-DEMO staged design approach in the pre-concept design phase, Fusion Eng. Des. 173 (2021) 112959.
[2] G. Caruso, S. Ciattaglia, B. Colling, L. Di Pace, D. Dongiovanni, M. D'Onorio, M. Garcia, X. Jin, J. Johnston, D. Leichtle, et al., DEMO–the main achievements of the pre–concept phase of the safety and environmental work package and the development of the GSSR, Fusion Eng. Des. 176 (2022) 113025.
[3] T. Pinna, D. Carloni, A. Carpignano, S. Ciattaglia, J. Johnston, M.T. Porfiri, L. Savoldi, N. Taylor, G. Sobrero, A. Uggenti, et al., Identification of accident sequences for the DEMO plant, Fusion Eng. Des. 124 (2017) 1277–1280.
[4] B. Merrill, R.L. Moore, S.T. Polkinghorne, D.A. Petti, Modifications to the MELCOR code for application in fusion accident analyses, Fusion Eng. Des. 51 (2000) 555–563.
[5] B. Merrill, Initial Modifications to the MELCOR Code, US ITER Participant Team Report, ITER/US/95/TE/SA-18, 1995, pp. 16–21.
[6] X.Z. Jin, BB LOCA analysis for the reference design of the EU DEMO HCPB blanket concept, Fusion Eng. Des. 136 (2018) 958–963.
[7] M. D'Onorio, F. Giannetti, M.T. Porfiri, G. Caruso, Preliminary safety analysis of an in-vessel LOCA for the EU-DEMO WCLL blanket concept, Fusion Eng. Des. 155 (2020) 111560.
[8] M. D'Onorio, T. Glingler, M.T. Porfiri, D.N. Dongiovanni, S. Ciattaglia, C. Gliss, J. Elbez-Uzan, P. Cortes, G. Caruso, Development of a thermal-hydraulic model for the EU-DEMO tokamak building and LOCA simulation, Energies 16 (3) (2023).
[9] F. Mascari, A. Bersano, M. Adorni, G. D'Ovidio, F. Martín-Fuertes, X. Jin, G. Mazzini, B. Gonfiotti, G. Georgiev, M. Leskovar, et al., Current status of MELCOR 2.2 for fusion safety analyses, Fusion Eng. Des. 194 (2023) 113869.
[10] B. Gonfiotti, S. Paci, Implementation and validation of a resuspension model in MELCOR 1.8. 6 for fusion applications, Fusion Eng. Des. 122 (2017) 64–85.
[11] M.D. Eklund, A.A. Riet, MELCOR-TMAP: The integration of MELCOR for fusion and TMAP4 for fusion reactor systems safety analysis and tritium inventory tracking, Fusion Eng. Des. 194 (2023) 113743.
[12] G. Federici, C. Bachmann, L. Barucca, W. Biel, L. Boccaccini, R. Brown, C. Bustreo, S. Ciattaglia, F. Cismondi, M. Coleman, et al., DEMO design activity in Europe: Progress and updates, Fusion Eng. Des. 136 (2018) 729–741.
[13] A. Del Nevo, P. Arena, G. Caruso, P. Chiovaro, P. Di Maio, M. Eboli, F. Edemetti, N. Forgione, R. Forte, A. Froio, et al., Recent progress in developing a feasible and integrated conceptual design of the WCLL BB in EUROfusion project, Fusion Eng. Des. 146 (2019) 1805–1809.
[14] V. Narcisi, A. Quartararo, I. Moscato, A. Santucci, Analysis of coolant purification strategies for tritium control in DEMO water primary coolant, Energies 16 (2) (2023) 617.
[15] G. Mazzini, T. Kaliatka, M.T. Porfiri, Estimation of tritium and dust source term in european DEMOnstration fusion reactor during accident scenarios, J. Nucl. Eng. Radiat. Sci. 5 (3) (2019) 030916.
[16] S. Ciattaglia, G. Federici, L. Barucca, M. de Magistris, E. Gaio, C. Gliss, M. Koerber, I. Moscato, M. Porfiri, F. Riedl, et al., Key EU DEMO plant and building layout criteria, Fusion Eng. Des. 171 (2021) 112567.
[17] G. Caruso, F. Giannetti, Sizing of the vacuum vessel pressure suppression system of a fusion reactor based on a water-cooled blanket, for the purpose of the preconceptual design, Sci. Technol. Nucl. Install. 2016 (1) (2016) 8719695.
[18] M. D'Onorio, G. Caruso, Pressure suppression system influence on vacuum vessel thermal-hydraulics and on source term mobilization during a multiple first wall–blanket pipe break, Fusion Eng. Des. 164 (2021) 112224.
[19] T. Glingler, G. Caruso, M. D'Onorio, Thermal-hydraulic optimization of a proposed EU-DEMO hydrogen passive removal system, Fusion Eng. Des. 194 (2023) 113729.
[20] G. Smolik, K. McCarthy, D. Petti, K. Coates, Hydrogen generation from steam reaction with Tungsten, J. Nucl. Mater. 258 (1998) 1979–1984.
[21] A. Bentaib, N. Meynet, A. Bleyer, Overview on hydrogen risk research and development activities: Methodology and open issues, Nucl. Eng. Technol. 47 (1) (2015) 26–32.
[22] L.L. Humphries, R.O. Gauntt, MELCOR 2.2 Severe Accident Analysis Code-Current Status and Plans for Future, Tech. rep., Sandia National Lab.(SNL-NM), Albuquerque, NM (United States), 2018.
[23] B.J. Merrill, Recent Updates to the MELCOR 1.8. 2 Code for ITER Applications, Tech. rep., Idaho National Lab.(INL), Idaho Falls, ID (United States), 2007.
[24] W.C. Hinds, Y. Zhu, Aerosol Technology: Properties, Behavior, and Measurement of Airborne Particles, John Wiley & Sons, 2022.
[25] K. McCarthy, D. Petti, W. Carmack, G. Smolik, The safety implications of tokamak dust size and surface area, Fusion Eng. Des. 42 (1–4) (1998) 45–52.